ECCOMAS Congress 2016
VII European Congress on Computational Methods in Applied Sciences and Engineering
M. Papadrakakis, V. Papadopoulos, G. Stefanou, V. Plevris (eds.)
Crete Island, Greece, 5–10 June 2016

SOME ACOUSTIC-TRANSPORT SPLITTING SCHEMES FOR TWO-PHASE COMPRESSIBLE FLOWS

Simon PELUCHON[1], Gérard GALLICE[2], and Pierre-Henri MAIRE[2]

[1] CEA-CESTA
15 avenue des Sablières, CS 60001, 33116 Le Barp cedex, FRANCE
e-mail: simon.peluchon@CEA.FR

[2] CEA-CESTA
15 avenue des Sablières, CS 60001, 33116 Le Barp cedex, FRANCE
e-mail: {gerard.gallice, pierre-henri.maire}@CEA.FR

Keywords: Compressible flow, Two-phase flow, Finite volume method, Carbuncle, Splitting operator.

Abstract. *In this paper, we present a splitting strategy to simulate compressible two-phase flows using the five-equation model [1]. The main idea of the splitting [2] is to separate the acoustic and transport phenomena. The acoustic step is solved as a Lagrangian step by using different schemes [3, 4, 5] based on approximate Riemann solvers. On the one hand, since the acoustic time step driven by the fast sound velocity is very restrictive, an implicit treatment of the Lagrangian step is performed. On the other hand, an explicit scheme is used for the transport step driven by the slow material waves. The global scheme resulting from this splitting operator strategy is conservative, positive, and preserves contact discontinuities. Numerical simulations of compressible diphasic flows are presented on 2d-structured grids. The implicit-explicit strategy allows large time steps, which do not depend on the fast acoustic waves.*

On supersonic velocity test case, a carbuncle phenomenon can occur with usual schemes for the Lagrangian part. However, we show that this carbuncle does not appear when the Lagrangian step is solved with a genuinely two-dimensional scheme based on a nine-point stencil [5].

1 INTRODUCTION

We are interested in solving compressible two-phase flows using a splitting strategy. Flows involving an almost incompressible liquid and a compressible gas are considered here. Using a diffuse interface approach [1, 6, 7], the same equations are solved in the entire domain. Therefore, the liquid is modelled by a compressible fluid in which the Mach number is very low. Several time scales are involved in this configuration: the scale of the fast acoustic waves which leads to an important CFL restriction of the time step for explicit schemes, and the scale of slow material waves.

In this paper, we propose an extension of the splitting strategy presented in [2, 8] to compressible two-phase flows using the five-equation system [1]. The splitting strategy is done with a Lagrange Projection algorithm. The acoustic part is solved in a Lagrangian form using several schemes [3, 5]. In Low Mach computations, an implicit treatment of this step should be done since the fast acoustic waves induce very small time steps. We are interested here in supersonic test cases, thus the acoustic step will be solved using an explicit scheme. The transport step is treated explicitly using a finite volume scheme.

The outline of this paper is as follow. In the second section we present the governing equations of two-phase flows. In section 3, the operator splitting in the one dimensional case is presented. We also describe the extension of the numerical scheme to two-dimensional structured grids in section 4. Several numerical schemes used in the Lagrangian part are recalled in section 5. Finally some numerical results for two-dimensional two-phase flows are presented in section 6. On supersonic computations, a carbuncle phenomenon appears with schemes based on a five-point stencil for the acoustic part. The shock instabilities disappear when a genuinely two-dimensional scheme is used in the acoustic step [5].

2 FIVE-EQUATION SYSTEM

We denote by ρ_i, ϵ_i and p_i the density, the internal energy and the pressure of the fluid phase $i = 1, 2$. Each fluid is equipped with an Equation Of State (EOS) of the form $p_i = p_i(\rho_i, \epsilon_i)$. The sound velocity c_i of each phase is defined by $c_i^2 = \frac{\partial p_i}{\partial \rho_i}\Big|_{s_i}$, where s_i is the entropy.

We introduce the volume fraction z_i of each fluid and we have the relation $z_1 + z_2 = 1$. In the sequel we denote by $z = z_1$ the volume fraction of the first fluid. The mixture density and mixture internal energy can be defined through the volume fraction, the density and internal energy of each fluid:

$$\rho = z_1\rho_1 + z_2\rho_2, \tag{1}$$
$$\rho\epsilon = z_1\rho_1\epsilon_1 + z_2\rho_2\epsilon_2. \tag{2}$$

Both phases share the same velocity $\mathbf{u}$, and the same pressure p. The five-equation system with isobaric closure derived in [1] reads:

$$\begin{aligned}
&\partial_t(\rho_1 z_1) + \nabla\cdot(\rho_1 z_1\mathbf{u}) = 0, \\
&\partial_t(\rho_2 z_2) + \nabla\cdot(\rho_2 z_2\mathbf{u}) = 0, \\
&\partial_t(\rho\mathbf{u}) + \nabla\cdot(\rho\mathbf{u}\otimes\mathbf{u}) + \nabla p = 0, \\
&\partial_t(\rho e) + \nabla\cdot((\rho e + p)\,\mathbf{u}) = 0, \\
&\partial_t z + \mathbf{u}\cdot\nabla z = 0, \\
&p = p_1 = p_2,
\end{aligned} \tag{3}$$

where $e = \epsilon + \frac{\mathbf{u}^2}{2}$ is the total energy of the mixture.

The evolution of the volume fraction is governed by a non-conservative equation. This formulation preserves contact discontinuities, i.e. the evolution of constant pressure and velocity profiles, see [1].

We only consider here a stiffened gas EOS for each fluid,

$$p_i = \rho_i \epsilon_i \left(\gamma_i - 1\right) - \gamma_i \pi_i, \tag{4}$$

where $\gamma_i > 1$ is the adiabatic exponent and $\pi_i \geq 0$ a reference pressure.

The mixture pressure of two stiffened gases is $p = \left(\gamma - 1\right)\rho\epsilon - \gamma\pi$ where the mixture parameters γ and π are defined by:

$$\gamma = 1 + \frac{1}{\sum_{i=1}^{2} \frac{z_i}{\gamma_i - 1}} \quad \text{and} \quad \pi = \frac{\gamma - 1}{\gamma} \sum_{i=1}^{2} \frac{z_i \gamma_i \pi_i}{\gamma_i - 1}. \tag{5}$$

The speed of sound for a stiffened gas reads:

$$c_i^2 = \gamma_i \frac{p + \pi_i}{\rho_i}.$$

3 SPLITTING STRATEGY FOR ONE DIMENSIONAL CASE

For the sake of simplicity, in this section a one dimensional problem is considered. The idea is to separate the acoustic and the transport phenomena according to their own propagation speed [2]. First, note that the evolution equation of $\rho_2 z_2$ in (3) can be replaced by the evolution equation of the mixture density ρ which is $\partial_t \rho + \partial_x(\rho u) = 0$. Then, the system (3) is expanded to:

$$\begin{aligned}
\partial_t \rho + \rho \partial_x u + u \partial_x \rho &= 0, \\
\partial_t \left(\rho_1 z\right) + \rho_1 z \partial_x u + u \partial_x (\rho_1 z) &= 0, \\
\partial_t \left(\rho u\right) + \rho u \partial_x u + \partial_x p + u \partial_x (\rho u) &= 0, \\
\partial_t \left(\rho e\right) + \rho e \partial_x u + \partial_x \left(p u\right) + u \partial_x (\rho e) &= 0, \\
\partial_t z + u \partial_x z &= 0.
\end{aligned} \tag{6}$$

This system is split into the following two systems. The first system takes into account the propagation of the acoustic waves only:

$$\begin{aligned}
\partial_t \rho + \rho \partial_x u &= 0, \\
\partial_t \left(\rho_1 z\right) + \rho_1 z \partial_x u &= 0, \\
\partial_t \left(\rho u\right) + \rho u \partial_x u + \partial_x p &= 0, \\
\partial_t \left(\rho e\right) + \rho e \partial_x u + \partial_x \left(p u\right) &= 0, \\
\partial_t z &= 0.
\end{aligned} \tag{7}$$

The transport system takes into account the propagation of the material waves through the fluid:

$$\begin{aligned}
\partial_t \rho + u \partial_x \rho &= 0, \\
\partial_t \left(\rho_1 z_1\right) + u \partial_x \left(\rho_1 z_1\right) &= 0, \\
\partial_t \left(\rho u\right) + u \partial_x \left(\rho u\right) &= 0, \\
\partial_t \left(\rho e\right) + u \partial_x \left(\rho e\right) &= 0, \\
\partial_t z + u \partial_x z &= 0.
\end{aligned} \tag{8}$$

The overall algorithm for a time step between t^n and t^{n+1} reads:

Step 1: From a state $(\rho, \rho_1 z, \rho u, \rho e, z)^n$, compute the approximation of the acoustic system (7) $(\rho, \rho_1 z, \rho u, \rho e, z)^{n+1,L}$.

Step 2: Find the fluid state $(\rho, \rho_1 z, \rho u, \rho e, z)^{n+1}$ by solving the transport system (8) with the initial state $(\rho, \rho_1 z, \rho u, \rho e, z)^{n+1,L}$.

Before going any further, we introduce some classical notations. We consider a discretization of the real line into cells $\Big([x_{i-1/2}, x_{x+1/2}]\Big)_{i\in Z}$. The mesh interfaces are $x_{i+1/2} = i\Delta x$ for $i \in Z$, where $\Delta x > 0$ is the grid step. The centre of the cell i is $x_i = \frac{x_{i+1/2}+x_{i-1/2}}{2}$. The time variable is discretized by $t^n = n\Delta t$ for $n \in N$, where $\Delta t > 0$ is the time step. We use a Finite Volume method, in which a_i^n is the approximation of

$$\frac{1}{\Delta x}\int_{x_{i-1/2}}^{x_{i+1/2}} a(x, t^n)\mathrm{d}x,$$

where $(x, t) \mapsto a(x, t)$ is a fluid parameter.

3.1 Acoustic step

First, the non-conservative system (7) is rearranged. The second, third and fourth equations of acoustic system are combined with the evolution equation of the mixture density. Then, the first equation is divided by the mixture density. Finally, the acoustic system reads:

$$\begin{aligned}
\partial_t \vartheta - \frac{1}{\rho}\partial_x u &= 0, \\
\partial_t y &= 0, \\
\partial_t u + \frac{1}{\rho}\partial_x p &= 0, \\
\partial_t e + \frac{1}{\rho}\partial_x (pu) &= 0, \\
\partial_t z &= 0,
\end{aligned} \tag{9}$$

where $\vartheta = \frac{1}{\rho}$ is the specific volume, and $y = \frac{\rho_1 z}{\rho}$ is the mass fraction of fluid 1.

Let us introduce the mass variable m defined by $\mathrm{d}m = \rho \mathrm{d}x$. The acoustic step consists in resolving a hyperbolic system of the form

$$\partial_t V + \partial_m G(V) = 0, \tag{10}$$

with $V = {}^t(\vartheta, y, u, e, z)$ and $G = {}^t(-u, 0, p, pu, 0)$.

This system is strictly hyperbolic and the five real eigenvalues are $(\lambda_1, \lambda_2, \lambda_3, \lambda_4, \lambda_5) = (-\rho c, 0, 0, 0, \rho c)$. Let us denote by $a = \rho c$ the Lagrangian speed of sound. The first and the fifth characteristic fields are genuinely non-linear while the waves associated to λ_2, λ_3 and λ_4 are linearly degenerate.

A classical approach to solve hyperbolic system like (10) is to use a Godunov type scheme. The update formula for the Lagrangian step reads

$$V_i^{n+1,L} = V_i^n - \frac{\Delta t}{\Delta m_i}\left(H_{i+1/2}^n - H_{i-1/2,}^n\right), \tag{11}$$

where $H = {}^t\Big(h^{(1)}, 0, h^{(3)}, h^{(4)}, 0\Big)$ is the numerical flux, and $\Delta m_i = \rho_i^n \Delta x$.

In the sequel, we use introduce the notation $[\![x]\!]_i = x_{i+1/2} - x_{i-1/2}$ for any quantity $(x_{i+1/2})_i$ defined at an interface.

The update formulae for the Eulerian variables are directly given by:

$$\begin{aligned}
&L_i \rho_i^{n+1,L} = \rho_i^n, \\
&L_i \left(\rho_1 z\right)_i^{n+1,L} = \left(\rho_1 z\right)_i^n, \\
&L_i \left(\rho u\right)_i{}^{n+1,L} = (\rho u)_i^n - \frac{\Delta t}{\Delta x}[\![h^{(3)}]\!]_i, \\
&L_i \left(\rho e\right)_i{}^{n+1,L} = (\rho e)_i^n - \frac{\Delta t}{\Delta x}[\![h^{(4)}]\!]_i, \\
&z_i^{n+1,L} = z_i^n,
\end{aligned} \tag{12}$$

with $L_i = 1 + \frac{\Delta t}{\Delta x}[\![-h^{(1)}]\!]_i$.

The acoustic step is stable under the classical Courant-Friedrichs-Lewy stability condition, given by

$$\frac{\Delta t}{\Delta x} \max_{i \in Z} \left(\frac{a_{i+1/2}}{\min(\rho_i^n, \rho_{i+1}^n)} \right) \leq \frac{1}{2}. \tag{13}$$

where $a_{i+1/2}$ is the Lagrangian sound speed at the interface $i + 1/2$.

3.2 Transport step

The transport system (8) is a convection system at the fluid velocity u. Therefore, it is simply approximated by an upwind Finite Volume scheme:

$$\phi_i^{n+1} = \phi_i^{n+1,L} - \frac{\Delta t}{\Delta x} \left(\left(\tilde{u}_{i+1/2}\right)^- \left(\phi_{i+1}^{n+1,L} - \phi_i^{n+1,L}\right) + \left(\tilde{u}_{i-1/2}\right)^+ \left(\phi_i^{n+1,L} - \phi_{i-1}^{n+1,L}\right) \right), \tag{14}$$

where ϕ denotes $\rho, \rho_1 z, \rho u, \rho e, z$, and with the classical notation $u^{\pm} = \frac{u \pm |u|}{2}$.

In order to have a fully conservative scheme for $\rho, \rho_1 z, \rho u$ and ρe, the choice of the propagation velocity $\tilde{u}_{i+1/2}$ should depend on the flux of the acoustic step.
Indeed, let us rewrite (14) as

$$\phi_i^{n+1} = \phi_i^{n+1,L} \left(1 + \frac{\Delta t}{\Delta x}[\![\tilde{u}]\!]_i\right) - \frac{\Delta t}{\Delta x}[\![\phi^{n+1,L}\tilde{u}]\!]_i,$$

where $\phi_{i+1/2}^{n+1,L}$ is defined as the upwind value of ϕ with respect to the sign of the velocity $\tilde{u}_{i+1/2}$, i.e. $\phi_{i+1/2}^{n+1,L} = \phi_i^{n+1,L}$ if $\tilde{u}_{i+1/2} > 0$, and $\phi_{i+1}^{n+1,L}$ otherwise.

We also denote by $\tilde{L}_i$ the volume variation $1 + \frac{\Delta t}{\Delta x}[\![\tilde{u}]\!]_i$. Combining this equation with explicit formulae (12) for the acoustic step, one can see that the overall scheme to compute the state at the time t^{n+1} from the state at t^n reads:

$$\begin{aligned}
\rho_i^{n+1} &= \frac{\tilde{L}_i}{L_i}\rho_i^n - \frac{\Delta t}{\Delta x}[\![\tilde{u}\rho^{n+1,L}]\!]_i, \\
(\rho_1 z)_i^{n+1} &= \frac{\tilde{L}_i}{L_i}(\rho_1 z)_i^n - \frac{\Delta t}{\Delta x}\left([\![\tilde{u}(\rho_1 z)^{n+1,L}]\!]_i\right), \\
(\rho u)_i^{n+1} &= \frac{\tilde{L}_i}{L_i}(\rho u)_i^n - \frac{\Delta t}{\Delta x}\left([\![\tilde{u}(\rho u)^{n+1,L}]\!]_i + \frac{\tilde{L}_i}{L_i}[\![h^{(3)}]\!]_i\right),
\end{aligned} \tag{15}$$

$$(\rho e)_i^{n+1} = \frac{\tilde{L}_i}{L_i}(\rho e)_i^n - \frac{\Delta t}{\Delta x}\left(\llbracket \tilde{u}(\rho e)^{n+1,L} \rrbracket_i + \frac{\tilde{L}_i}{L_i}\llbracket h^{(4)} \rrbracket_i\right),$$
$$z_i^{n+1} = z_i^{n+1,L} + \frac{\Delta t}{\Delta x}\llbracket h^{(1)} z^n \rrbracket_i - z_i^n \frac{\Delta t}{\Delta x}\llbracket h^{(1)} \rrbracket_i.$$

One can see that the global scheme is conservative if $\tilde{L}_i = L_i$. This choice leads to define the propagation velocity at an interface as the opposite of the first component of the acoustic flux:

$$\tilde{u}_{i+1/2} = -h^{(1)}_{i+1/2}. \tag{16}$$

With this choice, the global scheme reads:

$$\begin{aligned}
\rho_i^{n+1} &= \rho_i^n + \frac{\Delta t}{\Delta x}\llbracket h^{(1)} \rho^{n+1,L} \rrbracket_i, \\
(\rho_1 z)_i^{n+1} &= (\rho_1 z)_i^n + \frac{\Delta t}{\Delta x}\llbracket h^{(1)} (\rho_1 z)^{n+1,L} \rrbracket_i, \\
(\rho u)_i^{n+1} &= (\rho u)_i^n + \frac{\Delta t}{\Delta x}\llbracket h^{(1)} (\rho u)^{n+1,L} - h^{(3)} \rrbracket_i, \\
(\rho e)_i^{n+1} &= (\rho e)_i^n + \frac{\Delta t}{\Delta x}\llbracket h^{(1)} (\rho e)^{n+1,L} - h^{(4)} \rrbracket_i, \\
z_i^{n+1} &= z_i^n + \frac{\Delta t}{\Delta x}\llbracket h^{(1)} z^n \rrbracket_i - z_i^n \frac{\Delta t}{\Delta x}\llbracket h^{(1)} \rrbracket_i.
\end{aligned} \tag{17}$$

It is fully conservative with respect to $\rho, \rho_1 z, \rho u, \rho e$, but not for the color function equation.

The stability condition associated with this transport step reads

$$\frac{\Delta t}{\Delta x} \max_{i \in R} \left(\tilde{u}^+_{i-1/2} - \tilde{u}^-_{i+1/2} \right) < 1. \tag{18}$$

4 EXTENSION TO TWO DIMENSIONS

Without loss of generality, a two dimensional problem discretized over a structured mesh is considered. Let us denote by $\Omega_{l,m}$ a cell of our mesh, $\Gamma_{l+1/2,m}$ (resp. $\Gamma_{l,m+1/2}$) the face of the cell $\Omega_{l,m}$ toward the direction x (resp. y) and $\vec{n}_{l+1/2,m}$ the unit vector normal to $\Gamma_{l+1/2,m}$, see Fig. 1.

System (3) is again split into two parts. The first part is the acoustic step:

$$\begin{aligned}
\partial_t \rho + \rho \nabla \cdot \mathbf{u} &= 0, \\
\partial_t (\rho_1 z) + \rho_1 z \nabla \cdot \mathbf{u} &= 0, \\
\partial_t (\rho \mathbf{u}) + \rho \mathbf{u} \nabla \cdot \mathbf{u} + \nabla \cdot p &= 0, \\
\partial_t (\rho e) + \rho e \nabla \cdot \mathbf{u} + \nabla \cdot (p \mathbf{u}) &= 0, \\
\partial_t z &= 0.
\end{aligned} \tag{19}$$

The second system is the transport step:

$$\begin{aligned}
\partial_t \rho + \mathbf{u} \cdot \nabla \rho &= 0, \\
\partial_t (\rho_1 z) + \mathbf{u} \cdot \nabla (\rho_1 z) &= 0, \\
\partial_t (\rho \mathbf{u}) + \mathbf{u} \cdot \nabla (\rho \mathbf{u}) &= 0, \\
\partial_t (\rho e) + \mathbf{u} \cdot \nabla (\rho e) &= 0, \\
\partial_t z + \mathbf{u} \cdot \nabla z &= 0.
\end{aligned} \tag{20}$$

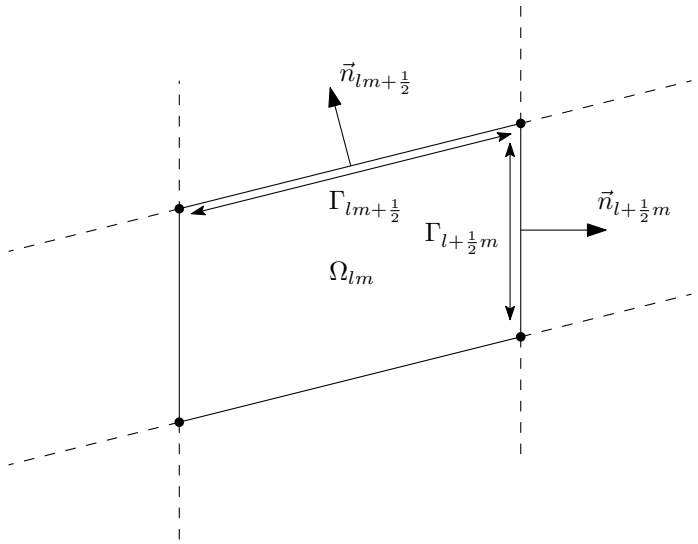

Figure 1: Parameters of a cell in two dimensions.

For any quantity x defined at a cell interface, let us introduce the following notations

$$[\![x_{.m}]\!]_l = x_{l+1/2,m} - x_{l-1/2,m},$$
$$[\![x_{l.}]\!]_m = x_{l,m+1/2} - x_{l,m-1/2}.$$

The volume of a cell $\Omega_{l,m}$ is denoted by $|\Omega_{l,m}|$. Likewise, the length of a face $\Gamma_{l+1/2,m}$ is denoted by $\left|\Gamma_{l+1/2,m}\right|$.

If a is a flow parameter, $a^n_{l,m}$ is an approximation of $\frac{1}{|\Omega_{l,m}|}\int_{\Omega_{l,m}} a(\mathbf{x}, t^n)\mathrm{d}\mathbf{x}$.

Acoustic step: Like in the one dimensional case, the scheme for the acoustic step reads

$$V^{n+1,L}_{l,m} = V^n_{l,m} - \frac{\Delta t}{\rho^n_{l,m}\,|\Omega_{l,m}|}\left([\![H_{.m}\,|\Gamma_{.m}|]\!]_l + [\![H_{l.}\,|\Gamma_{l.}|]\!]_m\right), \tag{21}$$

where $V = {}^t(\vartheta, y, \mathbf{u}, e, z)$ and $H_{l+1/2,m} = H(V_{l,m}, V_{l+1,m})$.

Transport step: For $\phi \in \{\rho, \rho_1 z, \rho\mathbf{u}, \rho e, z\}$, the scheme for the transport step reads:

$$\begin{aligned}\phi^{n+1}_{l,m} &= \phi^{n+1,L}_{l,m}\left(1 - \frac{\Delta t}{|\Omega_{l,m}|}\left([\![h^{(1)}_{.m}\,|\Gamma_{.m}|]\!]_l + [\![h^{(1)}_{l.}\,|\Gamma_{l.}|]\!]_m\right)\right) \\ &+ \frac{\Delta t}{|\Omega_{l,m}|}\left([\![h^{(1)}_{.m}\phi^{n+1,L}_{.m}\,|\Gamma_{.m}|]\!]_l + [\![h^{(1)}_{l.}\phi^{n+1,L}_{l.}\,|\Gamma_{l.}|]\!]_m\right)\end{aligned} \tag{22}$$

5 NUMERICAL FLUXES FOR THE ACOUSTIC STEP

In this section, different Lagrangian schemes used in the acoustic step are defined. The first one uses a classical five-point stencil while the second one is based on a nine-point stencil.

5.1 Scheme based on a five-point stencil

We consider the Lagrangian scheme developed in [3] for the gas dynamics. This Godunov-type scheme based on a simple Riemann solver, see Fig. 2, is positive, entropic and preserves contact discontinuities.

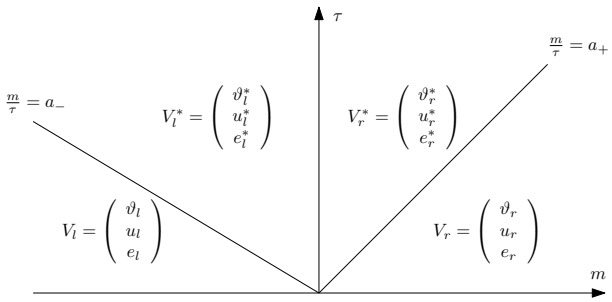

Figure 2: Five-point scheme. Riemann solver.

For gas dynamics, [3] shows that the numerical flux H is equal to the continuous flux G evaluated at an average state:

$$H\left(V_l, V_r\right) = {}^t(-\bar{u}, 0, \bar{p}\vec{n}, \bar{p}\bar{u}, 0)\,, \tag{23}$$

where the velocity and the pressure at the interface between the cells Ω_l and Ω_r are defined by:

$$\begin{aligned} \bar{u} &= \frac{a_-\mathbf{u}_l + a_+\mathbf{u}_r}{a_- + a_+} \cdot \vec{n} - \frac{p_r - p_l}{a_- + a_+}, \\ \bar{p} &= \frac{a_+p_l + a_-p_r}{a_- + a_+} - a_-a_+\frac{\mathbf{u}_r - \mathbf{u}_l}{a_- + a_+} \cdot \vec{n}. \end{aligned} \tag{24}$$

The Lagrangian sound velocities at the interface a_- and a_+ should be large enough in order to preserve the positivity of the scheme, see [3] for more details.

Remark: To compute an implicit scheme for the acoustic step, we use the method described in [2].

5.2 Scheme based on a nine-point stencil

Another choice for the Lagrangian part is to use the scheme developed in [5] for gas dynamics. In this case, fluxes computations are based on a nodal solver.

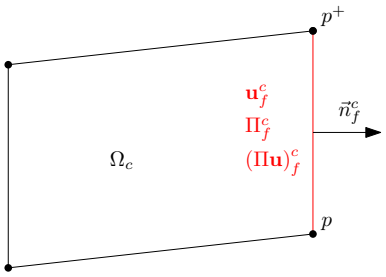

Figure 3: Nine-point scheme. Notations related to the cell Ω_c.

The numerical flux on the face $f = [p, p^+]$ of the cell Ω_c (see Fig. 3) is defined as:

$$H(f) = (\mathbf{u}_f^c \cdot \vec{n}_f^c, 0, \Pi_f^c\vec{n}_f^c, (\Pi\mathbf{u})_f^c \cdot \vec{n}_f^c, 0), \tag{25}$$

where

$$\mathbf{u}_f^c = \frac{1}{2}(\mathbf{u}_p + \mathbf{u}_{p^+}),$$

$$\Pi_f^c = \frac{1}{2}(\Pi_{\bar{p}}^c + \Pi_{\underline{p}^+}^c),$$
$$(\Pi \mathbf{u})_f^c = \frac{1}{2}(\Pi_{\bar{p}}^c \mathbf{u}_p + \Pi_{\underline{p}^+}^c \mathbf{u}_{p^+}).$$

The velocity and pressure on the face f are defined through the nodal velocities $\mathbf{u}_p$ and $\mathbf{u}_{p^+}$, and the nodal pressures, $\Pi_{\bar{p}}^c$ and $\Pi_{\underline{p}^+}^c$, see Fig. 4. The evaluation of these nodal quantities relies on an argument of conservation concerning both momentum and total energy. The nodal pressures are linked to the nodal velocity thanks to half-Riemann problems. Since the nodal velocity $\mathbf{u}_p$ depends of all the cells around the node p, the resulting scheme is based on a nine-point stencil.

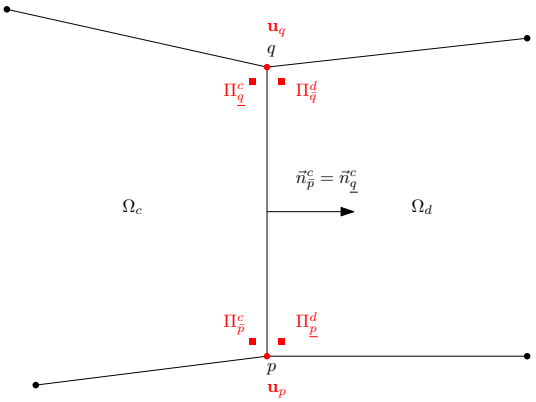

Figure 4: Nine-point scheme. Nodal velocities and pressures related to the face $[p, q]$

6 NUMERICAL RESULTS

In this section, several numerical experiments are presented in order to validate the splitting strategy and compare the different solvers used in the acoustic step.

6.1 Liquid-gas interaction

First, a classical two dimensional test case is considered. The interaction between a bubble of gas and a liquid has already been investigated in [7, 9].

The computational domain is a rectangle of size $L_x = 2$m and $L_y = 1$m described in Fig. 5. The gas is contained in a bubble of radius 0.4m located at the position $(0.5m, 0.5m)$. The shock area is delimited by $x < 0.04$m. Initial conditions are gathered in Table 1.

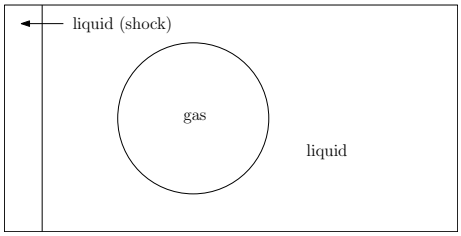

Figure 5: Liquid-gas interaction: description of the computational domain

	Density (kg m^{-3})	Pressure (Pa)	Velocity (m s^{-1})	γ	π (Pa)
Liquid (shock)	1030.9	3×10^9	$(300., 0.)$	4.4	6.8×10^8
Liquid	1000.	10^5	$(0., 0.)$	4.4	6.8×10^8
Gas	1.	10^5	$(0., 0.)$	1.4	0

Table 1: Liquid-gas interaction. Initial conditions.

A 600×300 space grid is used for the numerical computation. Wall boundary conditions are imposed on the upper and lower sides, and input/output boundary conditions on the other sides. The Courant number is 0.5.

The mapping of the volume fraction is plotted at several times in Fig. 6 and Fig. 7. Results show good agreement between the two solvers. We also note that our results are similar to those presented in [7] or [9].

Figure 6: Liquid-gas interaction. Mapping of the volume fraction z after 125 μs and 600 μs for the five-point stencil scheme [3]

Figure 7: Liquid-gas interaction. Mapping of the volume fraction z after 125 μs and 600 μs for the nine-point stencil scheme [5].

Remark: With the five-point-stencil scheme, the use of an implicit scheme in the acoustic part reduces the computational time by 34.

6.2 Steady supersonic flow over a cylinder

A Mach 10 steady flow over a cylinder is considered. The radius of the cylinder is equal to 1. The computational domain is covered by a 100×200 structured grid. We note that this case is monophasic.

A comparison between the two solvers for the Lagrangian step defined in section 5 is done, see Fig. 8. With the five-point stencil scheme, carbuncle phenomenon appears near the stagnation point. The numerical solution is not symmetrical. We note that the shape of the shock instabilities is not similar to those presented in the literature [10, 11, 12]. With the genuinely two-dimensional scheme, the solution is perfectly acceptable. Similar results have been presented in [11], where a nine-point scheme eliminates shock instabilities.

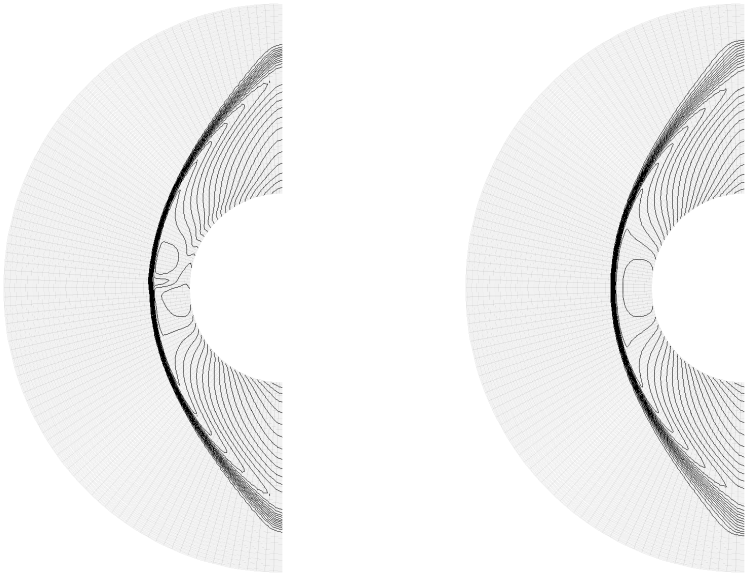

Figure 8: Mach 10 flow over a cylinder: density contours. Comparison between different solvers in the acoustic step. Left: five-point stencil from [3], Right: nine-point solver from [5].

Usually, such computations are done with direct Eulerian finite volume methods. In this case, a possible cure for the carbuncle phenomenon is to use of a dissipative scheme, like the HLL scheme [4]. Indeed these schemes are very robust for supersonic computation involving shocks but they are very dissipative in the boundary layer. Another approach is to use a combination of a dissipative flux function and a classical scheme [12].

In our splitting strategy, we used the HLL scheme for the acoustic step. One can see in Fig. 9 that carbuncle still appears.

Using the splitting strategy, carbuncle phenomenon seems to appear with all schemes based on a five-point stencil. However, the scheme based on a nine-point stencil in the Lagrangian part might offer a cure for carbuncle.

6.3 Interaction of supersonic gas flow with a liquid droplet

Finally, a unsteady supersonic two-phase flow test case is presented. We are interested in the interaction between a supersonic gas flow and a liquid droplet.

We consider a 5 mm$\times 3$ mm rectangular domain. A liquid droplet of radius $r = 0.25$ mm is initially located at the position $(1, 0)$ mm. The droplet is modelled by a stiffened gas with the coefficients $\gamma = 4.4$ and $\pi = 6.10^8$ Pa. The liquid is initially at rest, with a density of 1000 kg.m^{-3} at the atmospheric pressure. The gas flow is considered as a perfect gas with $\gamma = 1.4$. At the initial time, the gas density is equal to 1.293 kg.m^{-3}, $\mathbf{u} = (5000, 0)$ m.s^{-1}, and the pressure is 10^5 Pa.

The mapping of the fluid velocity magnitude for both solvers is plotted in Fig. 10. The position of the bow shock is the same with the two solvers. In Fig. 10, the black line represents the geometry of the liquid droplet. One can see that the location of droplet is the same but the shape is different.

The velocity contours are plotted in Fig. 11. One can see that carbuncle phenomenon also appears in this two-phase flow test case with the five-point stencil scheme. It seems to disturb the gas flow between the bow shock and the liquid droplet. With the genuinely two-dimensional

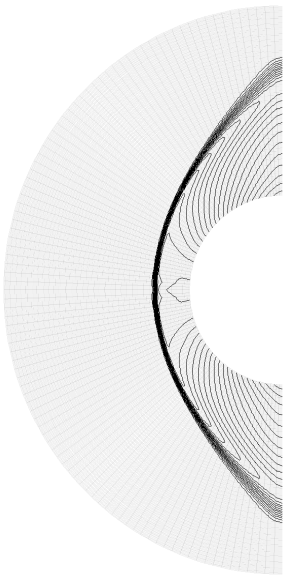

Figure 9: Mach 10 flow over a cylinder: density contours with HLL solver.

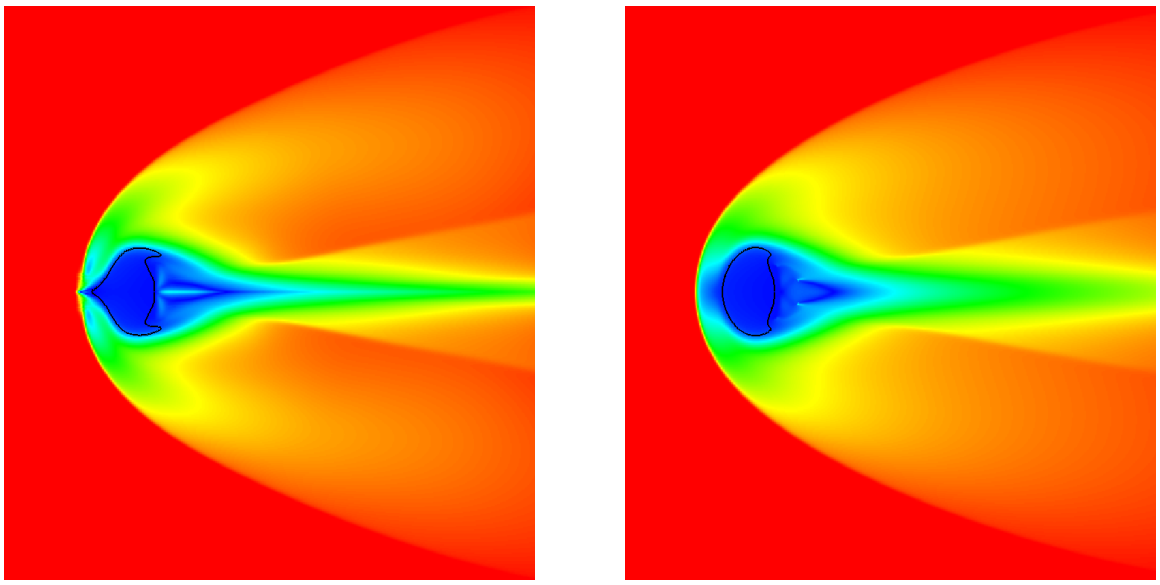

Figure 10: Interaction of supersonic gas flow with a liquid droplet. Mapping of the fluid velocity magnitude and contour of the liquid droplet (in black) after 1.57 μs. Left: five-point stencil from [3], Right: nine-point solver from [5].

scheme, there are no instabilities between the bow shock and the droplet. The scheme based on a nine-point stencil did not allow the carbuncle to appear even in this diphasic test case.

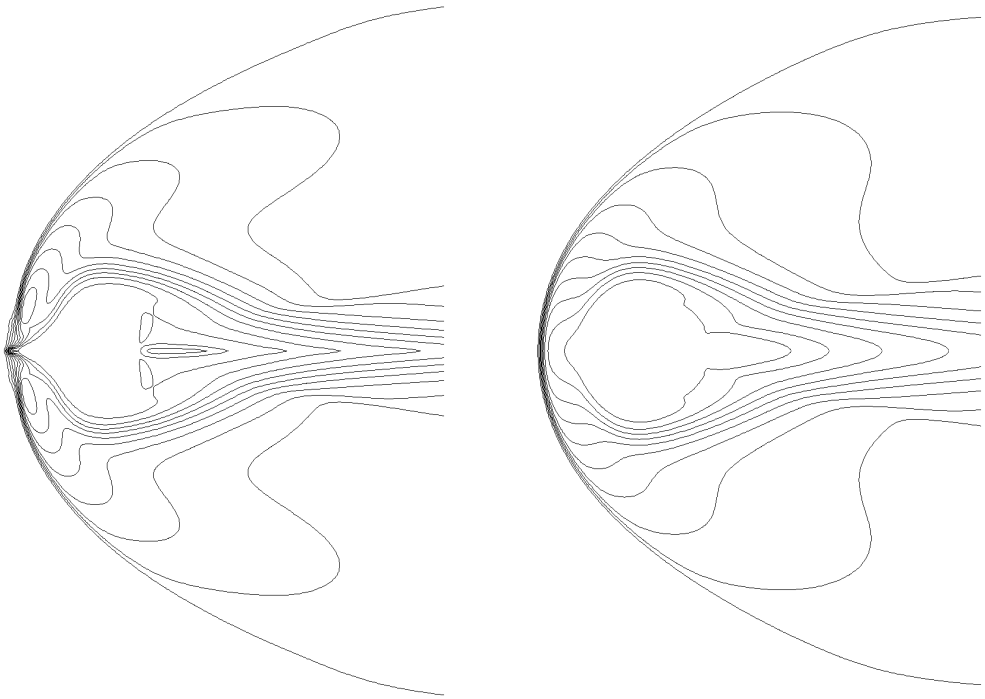

Figure 11: Interaction of supersonic gas flow with a liquid droplet. Velocity contour after 1.57 μs. Left: five-point stencil from [3], Right: nine-point solver from [5].

7 CONCLUSIONS

In this present work, an extension of the operator splitting strategy [2, 8] to two-phase flows using the five-equation model [1] have been presented. This strategy decouples acoustic and transport phenomena. Several schemes based on five-point or nine-point stencils are used in the acoustic step. In non-supersonic numerical simulations, the different schemes produce the same results. On supersonic velocity test case, carbuncle phenomenon appears with the five-point scheme. Using a very dissipative scheme like HLL in the Lagrangian part of the splitting does not prevent the apparition of the instabilities. However, carbuncle does not appear when the acoustic step is solved with a genuinely two-dimensional scheme based on a nine-point stencil.

In the future, the implicit scheme for the genuinely two-dimensional scheme based on a nine-point stencil has to be developed. The extension to Navier-Stokes equations is already in progress. Finally, the extension of the genuinely two-dimensional scheme based on an approximate Riemann solver located at the node in direct Eulerian approach will be considered.

REFERENCES

[1] G. Allaire, S. Clerc, S. Kokh, A Five-Equation Model for the Simulation of Interfaces between Compressible Fluids. *Journal of Computational Physics*, **181**, 577–616, 2002.

[2] C. Chalons, M. Girardin, S. Kokh, An all-regime Lagrange-Projection like scheme for gas dynamics equations on unstructured meshes. *submitted*, 2014.

[3] G. Gallice, Positive and Entropy Stable Godunov-type Schemes for Gas Dynamics and MHD Equations in Lagrangian or Eulerian Coordinates. *Numerische Mathematik*, **94**, 673–713, 2003.

[4] A. Harten, P.D. Lax, B. van Leer, On upstream differencing and Godunov-type schemes for hyperbolic conservation laws. *SIAM review*, **25**, 35–61, 1983

[5] P-H. Maire, A high-order cell-centered Lagrangian scheme for two-dimensional compressible fluid flows on unstructured meshes. *Journal of Computational Physics*, **228**, 2391–2425, 2009.

[6] MR. Baer, JW. Nunziato, A two-phase mixture theory for the deflagration-to-detonation transition (DDT) in reactive granular materials. *International journal of multiphase flow*, **12**, 861–889, 1986.

[7] R. Saurel, R. Abgrall, A simple method for compressible multifluid flows. *SIAM J. Sci. Comput.*, **21**(3), 1115–1145, 1999.

[8] C. Chalons, M. Girardin, S. Kokh, An all-regime Lagrange-Projection like scheme for 2D homogeneous models for two-phase flows on unstructured meshes. *submitted*, 2014.

[9] S. Kokh, F. Lagoutière, An anti-diffusive numerical for the simulation of interfaces between compressible fluids by means of five-equation model. *Journal of Computational Physics*, **229**, 2773–2809, 2010.

[10] Y. Chauvat, J.-M. Moschetta and J. Gressier, Shock wave numerical structure and the carbuncle phenomenon. *International Journal for Numerical Methods in Fluids*, **47**, 903–909, 2005

[11] Z. Shen, W. Yan et G. Yuan, A robust and contact resolving Riemann solver on unstructured mesh, Part I, Euler method. *Journal of Computational Physics*, **268**, 432–455, 2014.

[12] H. Nishikawa, K. Kitamura, Very simple, carbuncle-free, boundary-layer-resolving, rotated-hybrid Riemann solvers. *Journal of Computational Physics*, **227**, 2560–2581, 2008.